

REAL-TIME PARAMETER ESTIMATION IN THE FREQUENCY DOMAIN

Eugene A. Morelli

Research Engineer

NASA Langley Research Center

Hampton, Virginia USA 23681 – 2199

Abstract

A method for real-time estimation of parameters in a linear dynamic state space model was developed and studied. The application is aircraft dynamic model parameter estimation from measured data in flight for indirect adaptive or reconfigurable control. Equation error in the frequency domain was used with a recursive Fourier transform for the real-time data analysis. Linear and nonlinear simulation examples and flight test data from the F-18 High Alpha Research Vehicle (HARV) were used to demonstrate that the technique produces accurate model parameter estimates with appropriate error bounds. Parameter estimates converged in less than 1 cycle of the dominant dynamic mode natural frequencies, using control surface inputs measured in flight during ordinary piloted maneuvers. The real-time parameter estimation method has low computational requirements, and could be implemented aboard an aircraft in real time.

Nomenclature

A, B, C, D	system matrices
$E\{ \}$	expectation operator
g	acceleration due to gravity, ft/sec ²
h	altitude, ft
j	imaginary number = $\sqrt{-1}$
M	Mach number
N	total number of samples
Re	real part
R	measurement noise covariance matrix
t	time

V_t	true airspeed, ft/sec
x, u, y	state, input, and output vectors
z_i	measured output vector at time $i \Delta t$
α	angle of attack, rad
β	sideslip angle, rad
δ_a, δ_r	aileron, rudder deflections, rad
δ_e, δ_s	elevator, stabilator deflections, rad
δ_{ij}	Kronecker delta
v_i	discrete measurement noise vector
σ^2	variance
ω	angular frequency, rad/sec
θ	p -dimensional parameter vector

superscripts

T	transpose
\dagger	complex conjugate transpose
\sim	discrete Fourier transform
$\hat{}$	estimate
-1	matrix inverse

subscripts

i	value at time $i \Delta t$
o	trim or initial value

Introduction

Real-time identification of dynamic models is a requirement for indirect adaptive or reconfigurable control¹. One approach for satisfying this requirement is to assume the dynamic model has a linear structure with time-varying parameters to account for changes in the flight condition, stores, configuration, remaining fuel, or from various types of failures, wear, or damage. The task is then to identify accurate linear model parameter estimates from measured data in real time, so that the adaptive control logic can make the necessary

Copyright © 1999 by the American Institute of Aeronautics and Astronautics, Inc. No copyright is asserted in the United States under Title 17, U.S. Code. The U.S. Government has a royalty-free license to exercise all rights under the copyright claimed herein for Governmental purposes. All other rights are reserved by the copyright owner.

changes to the control law to achieve stability and performance goals.

Two main problems plague accurate real-time parameter estimation: noise and data information content. It is difficult to design a parameter estimation technique that is insensitive to noise but still responds rapidly to sudden changes in the system dynamics, mainly because it takes a fairly long data record to distinguish noise from a sudden change in the dynamics. This problem can be handled in the time domain using recursive least squares and a "forgetting factor"², or by using sequential batch least squares with short data records and including various constraints in the parameter estimation cost function^{3,4}. If an extended Kalman filtering approach⁵⁻⁸ is used, discriminating signal from noise is implemented through weighting matrices that represent assumed measurement and process noise covariances. For all of these time domain methods, some adjustment of one or more tuning parameters must be done in simulation. In addition, the standard errors for the model parameter estimates, which are important both for failure detection and adaptive or reconfigurable control, cannot be accurately and reliably computed using recursive or sequential batch time domain methods.

In the context of airplane flight, lack of information content in the data can be problematic because there are frequently extended periods where the control and state variables are fairly constant. Signal levels are at or below the (relatively constant) noise level. In this circumstance, a time domain regression method will give very inaccurate parameter estimates unless the estimation is regularized by including a term in the cost function that penalizes movement of the parameters away from some *a priori* known values (e.g., values from wind tunnel tests), and/or a term that penalizes time variation of the parameter estimates⁴. Tuning parameters are required for this approach, because the magnitude of the penalty term(s) must be balanced properly relative to the least squares part of the cost function used for parameter estimation based on measured data. Another problem that falls in the category of poor data information content is data collinearity due to the control system⁹. Many control laws move more than one control surface at the same time, or move control surfaces in proportion to state variables with a small time delay. When states and controls are nearly proportional to one another, it is impossible to identify individual stability and control derivatives from the measured data alone.

There are many parameter estimation methods, but the requirement of being simple enough to be

implemented in real time aboard the aircraft narrows the field. In particular, any method that iterates through the data must be eliminated. The current work is an investigation of a single-step frequency domain method for the real-time parameter estimation task, and an evaluation of its suitability for aircraft problems. This real-time parameter estimation method was first proposed as a component of a technique for in-flight system identification¹⁰. In the present work, the real-time parameter estimation method is developed further and applied to realistic simulation and flight test data.

The next section gives the problem statement and outlines the necessary theory. Following this, the real-time parameter estimation method is applied to a simulation example, where a linear truth model is used with outputs corrupted by noise similar to that seen in flight, and noise that is worse than usual. The application is identifying an accurate model for the longitudinal rigid body dynamics of a conventional fighter. The real-time parameter estimation procedure is further demonstrated with a longitudinal example using flight test data, and a nonlinear simulation example where both longitudinal and lateral/directional parameters are estimated.

Theoretical Development

Airplane dynamics can be described by the following linear model equations¹¹:

$$\dot{\mathbf{x}}(t) = \mathbf{A}\mathbf{x}(t) + \mathbf{B}\mathbf{u}(t) \quad (1)$$

$$\mathbf{x}(0) = \mathbf{x}_o \quad (2)$$

$$\mathbf{y}(t) = \mathbf{C}\mathbf{x}(t) + \mathbf{D}\mathbf{u}(t) \quad (3)$$

$$\mathbf{z}_i = \mathbf{y}_i + \mathbf{v}_i \quad i = 1, 2, \dots, N \quad (4)$$

Matrices \mathbf{A} , \mathbf{B} , \mathbf{C} , and \mathbf{D} in Eqs. (1) and (3) contain stability and control derivatives, which are assumed as constant model parameters to be estimated from flight data. Repeating the parameter estimation at short intervals produces piecewise constant estimates for time-varying model parameters in the linear model structure. The input quantities are control surface deflections (δ_e or δ_s , δ_a , δ_r), with the states selected from air data (V_t , α , β), body axis angular velocities (p , q , r), and Euler angles (ϕ , θ , ψ). Output

quantities can include the states and translational accelerations (a_x, a_y, a_z) .

Equation Error in the Frequency Domain

The finite Fourier transform of a signal $x(t)$ is defined by

$$\tilde{x}(\omega) \equiv \int_0^T x(t) e^{-j\omega t} dt \quad (5)$$

which can be approximated by

$$\tilde{x}(\omega) \approx \Delta t \sum_{i=0}^{N-1} x_i e^{-j\omega t_i} \quad (6)$$

Subscript i indicates the variable value at time $i \Delta t$, and Δt is the sampling interval. The summation in Eq. (6) is defined as the discrete Fourier transform,

$$X(\omega) \equiv \sum_{i=0}^{N-1} x_i e^{-j\omega t_i} \quad (7)$$

so that

$$\tilde{x}(\omega) \approx X(\omega) \Delta t \quad (8)$$

Some fairly straightforward corrections¹² can be made to Eq. (8) to remove the inaccuracy resulting from the fact that Eq. (8) is a simple Euler approximation to the finite Fourier transform of Eq. (5). However, if the sampling rate is much higher than the frequencies of interest (as is true in this case), then the corrections are small and can be safely ignored.

Applying the Fourier transform to Eqs. (1) and (3) gives

$$j\omega \tilde{\mathbf{x}}(\omega) = \mathbf{A} \tilde{\mathbf{x}}(\omega) + \mathbf{B} \tilde{\mathbf{u}}(\omega) \quad (9)$$

$$\tilde{\mathbf{y}}(\omega) = \mathbf{C} \tilde{\mathbf{x}}(\omega) + \mathbf{D} \tilde{\mathbf{u}}(\omega) \quad (10)$$

When the states, outputs, and inputs are measured, individual state or output equations from vector Eqs. (9) or (10) can be used in an equation error formulation to estimate the stability and control derivatives contained in matrices \mathbf{A} , \mathbf{B} , \mathbf{C} , and \mathbf{D} .

For the k th state equation of vector Eq. (9), the cost function is

$$J_k = \frac{1}{2} \sum_{n=1}^m \left| j\omega_n \tilde{x}_k(n) - \mathbf{A}_k \tilde{\mathbf{x}}(n) - \mathbf{B}_k \tilde{\mathbf{u}}(n) \right|^2 \quad (11)$$

where \mathbf{A}_k and \mathbf{B}_k are the k th rows of matrices \mathbf{A} and \mathbf{B} , respectively, and $\tilde{x}_k(n)$ is the k th element of vector $\tilde{\mathbf{x}}$ for frequency ω_n . Symbols $\tilde{\mathbf{x}}(n)$ and $\tilde{\mathbf{u}}(n)$ denote the Fourier transform of the state and control vectors for frequency ω_n . There are m terms in the summation, corresponding to m frequencies of interest, and each transformed variable depends on frequency. Similar cost expressions can be written for individual output equations from vector Eq. (10). Denoting the vector of unknown model parameters in \mathbf{A}_k and \mathbf{B}_k by θ , the problem can be formulated as a standard least squares regression problem with complex data,

$$\mathbf{Y} = \mathbf{X} \theta + \varepsilon \quad (12)$$

where

$$\mathbf{Y} \equiv \begin{bmatrix} j\omega_1 \tilde{x}_k(1) \\ j\omega_2 \tilde{x}_k(2) \\ \vdots \\ j\omega_m \tilde{x}_k(m) \end{bmatrix} \quad (13)$$

$$\mathbf{X} \equiv \begin{bmatrix} \tilde{\mathbf{x}}^T(1) & \tilde{\mathbf{u}}^T(1) \\ \tilde{\mathbf{x}}^T(2) & \tilde{\mathbf{u}}^T(2) \\ \vdots & \vdots \\ \tilde{\mathbf{x}}^T(m) & \tilde{\mathbf{u}}^T(m) \end{bmatrix} \quad (14)$$

and ε represents the complex equation error in the frequency domain. The least squares cost function is

$$J = \frac{1}{2} (\mathbf{Y} - \mathbf{X} \theta)^\dagger (\mathbf{Y} - \mathbf{X} \theta) \quad (15)$$

which is identical to the cost in Eq. (11). The parameter vector estimate that minimizes this cost function is computed from¹³

$$\hat{\theta} = \left[\text{Re}(\mathbf{X}^\dagger \mathbf{X}) \right]^{-1} \text{Re}(\mathbf{X}^\dagger \mathbf{Y}) \quad (16)$$

The estimated parameter covariance matrix is

$$\text{cov}(\hat{\theta}) \equiv E \left\{ (\hat{\theta} - \theta)(\hat{\theta} - \theta)^T \right\} = \sigma^2 \left[\text{Re}(\mathbf{X}^\dagger \mathbf{X}) \right]^{-1} \quad (17)$$

where the equation error variance σ^2 can be estimated from the residuals,

$$\hat{\sigma}^2 = \frac{1}{(m-p)} \left[(\mathbf{Y} - \mathbf{X}\hat{\theta})^\top (\mathbf{Y} - \mathbf{X}\hat{\theta}) \right] \quad (18)$$

and p is the number of elements in parameter vector θ . Parameter standard errors are computed as the square root of the diagonal elements of the $\text{cov}(\hat{\theta})$ matrix from Eq. (17), using $\hat{\sigma}^2$ from Eq. (18).

Recursive Fourier Transform

For a given frequency ω , the discrete Fourier transform in Eq. (7) at sample time i is related to the discrete Fourier transform at time $i-1$ by

$$X_i(\omega) = X_{i-1}(\omega) + x_i e^{-j\omega i \Delta t} \quad (19)$$

where

$$e^{-j\omega i \Delta t} = e^{-j\omega \Delta t} e^{-j\omega (i-1) \Delta t} \quad (20)$$

The quantity $e^{-j\omega \Delta t}$ is constant for a given frequency and constant sampling interval. It follows that the discrete Fourier transform can be computed for a given frequency at each time step using one addition in Eq. (19) and two multiplications – one in Eq. (20) using the stored constant $e^{-j\omega \Delta t}$ for frequency ω , and one in Eq. (19). There is no need to store the time domain data in memory when computing the discrete Fourier transform in this way, because each sampled data point is processed immediately. Time domain data from all preceding maneuvers can be used in all subsequent analysis by simply continuing the recursive calculation of the Fourier transform. In this sense, the recursive Fourier transform acts as memory for the information in the data. More data from more maneuvers improves the quality of the data in the frequency domain without increasing memory requirements to store it. In addition, the Fourier transform is available at any time $i \Delta t$. The approximation to the finite Fourier transform is completed using Eq. (8).

Rigid body dynamics of piloted aircraft lie in the rather narrow frequency band of approximately 0.01-1.5 Hz. It is therefore possible to select closely-spaced fixed frequencies for the Fourier transform and the subsequent data analysis. For all the examples studied in this work, frequency spacing of

0.04 Hz on the interval [0.1-1.5] Hz was found to be adequate, giving 36 evenly spaced frequencies for each transformed time domain signal. Excluding zero frequency removes trim values and measurement biases, so it is not necessary to estimate bias parameters. Using a limited frequency band for the Fourier transformation confines the data analysis to the frequency band where the system dynamics reside, and automatically filters wide band measurement noise or structural response outside the frequency band of interest.

For airplane dynamic modeling, the number of time domain signals to be transformed is usually low (9 or less – more if there are many control surfaces), so this approach requires a small amount of computer memory. Since the data analysis is done in the frequency domain, the memory required is fixed and independent of the time length of the flight maneuvers.

The recursive Fourier transform update need not be done for every sampled time point. Skipping some time points effectively decimates the data prior to Fourier transformation. This saves computation, and does not adversely impact the frequency domain data because the Nyquist frequency (equal to $\frac{1}{2}$ the sampling frequency) is usually much higher than the relatively low frequencies being used in the recursive Fourier transform.

Examples

For longitudinal aircraft short period dynamics, the state vector \mathbf{x} and input vector \mathbf{u} in Eq. (1) are defined by

$$\mathbf{x} = [\alpha \quad q]^\top \quad \mathbf{u} = [\delta_e] \quad (21)$$

System matrices containing the model parameters are:

$$\mathbf{A} = \begin{bmatrix} Z_\alpha & Z'_q \\ M_\alpha & M_q \end{bmatrix} \quad \mathbf{B} = \begin{bmatrix} Z_{\delta_e} \\ M_{\delta_e} \end{bmatrix} \quad (22)$$

The above model assumes $\dot{\alpha}$ effects can be subsumed into the Z'_q and M_q derivatives. Parameter Z'_q includes the inertial term, i.e., $Z'_q = 1 + Z_q$. In this and all the other examples, state equations were used for the equation error parameter estimation.

In the first example, a perturbation elevator input was applied to a known linear model to produce simulated state and output responses. Figure 1 shows the elevator input δ_e . The first 8 seconds of the

elevator input were taken from measured flight test data for a longitudinal tracking task. Constant elevator deflection is held for the final 7 seconds, to simulate low data information content. The simulated aircraft is a conventional F-16^{11,14} with forward c.g. position ($0.2 \bar{c}$) in straight and level trimmed flight at 10,000 ft, 7 deg angle of attack, and Mach 0.37. The simulated outputs were corrupted with 20% Gaussian random white noise. This made the signal-to-noise ratio 5-to-1 for each simulated output measurement. Figure 2 shows the simulated measured perturbation angle of attack α and pitch rate q . The elevator input was assumed to be measured without noise, which is a close approximation to reality. Model parameter values used to generate the simulated test data, called true values, are given in column 2 of Table 1. Parameter estimation was done in real time using equation error in the frequency domain applied to the two state equations, with the Fourier transform computed recursively, as described previously. All angular quantities were expressed in radians for the data analysis, but were plotted in degrees. Angular rates were expressed in radians per second for the data analysis, and plotted in degrees per second.

Figure 3 shows a time history of M_α model parameter estimates based on the simulated noisy data only. Plots for the other model parameters were similar. The model parameter estimates and standard errors were computed once a second using Eqs. (16)-(18) with frequency domain data from the recursive Fourier transform in Eqs. (19) and (20). This update rate for the parameter estimation was used throughout the examples, but was chosen arbitrarily. Parameter estimation updates can be done at a faster or slower rate, with the upper limit defined by the rate used in the recursive Fourier transform. The algorithm required no starting values for the parameters, and the estimates were not regularized in any way with *a priori* values or constraints on temporal changes in the parameter estimates. The first parameter estimates are shown at 2 seconds, because the parameter estimates after 1 second were poor with very large standard errors, due to the lack of information content in the data during the first second of the maneuver. Figure 3 shows that the parameter estimates converge to the true value. The calculated standard errors are representative of the estimated parameter accuracy throughout the maneuver, and do not suffer from the covariance wind-up problem characteristic of recursive time domain methods. Column 3 of Table 1 contains parameter estimates with corresponding standard errors in parentheses below. These results are for the end of the 15 second maneuver. Every parameter estimate is

within ± 1 standard error of the true value, indicating that the parameter estimation is accurate, and the estimated standard errors properly represent the true accuracy of the parameter estimates. The calculated standard errors accurately convey information on the quality of the parameter estimates throughout the maneuver, and do not become smaller with increasing maneuver time when there is no information in the data.

Figure 4 shows the same simulated model pitch rate output using the same input to the same model, but with the added Gaussian random noise level raised from 20% to 50%, reducing the signal-to-noise ratio to 2-to-1. In addition, two simulated data dropouts with values of -100 were added to the simulated pitch rate output. Plots in Figure 5 show that the parameter estimates in this case again converge to the true values, although the standard error values are generally higher, due to the increased noise level. Plots for the model parameters not shown were similar. The convergence rate of the parameter estimates to the true values was similar to the lower noise case, requiring approximately 4 seconds of data. This corresponds to approximately 1.4 periods of the short period natural frequency for the simulation model. Considering that no substantial information is contained in the data for the first two seconds, this is an excellent result. Discounting the first two seconds, the parameters were accurately estimated from approximately 2 seconds of data, corresponding to 0.7 cycles of the short period mode. The real-time parameter estimation algorithm is robust to measurement noise levels and infrequent data dropouts because of the automatic filtering inherent in using a limited bandwidth for the recursive Fourier transform. In effect, the data dropouts look the same as high frequency noise. Column 4 of Table 1 gives the parameter estimates and standard errors for the 50% noise case at the end of the 15 second maneuver. As before, every parameter estimate is within ± 1 standard error of the true value, indicating that the parameter estimates and standard errors are accurate.

The linear simulation and the real-time data analysis were programmed and run in MATLAB 5.3¹⁵. Sampling rate for the data was 40 Hz, and the recursive Fourier transform updates were done at 20 Hz. The real-time estimation algorithm ran roughly 10 times faster than real time (1.5 seconds for a 15 second maneuver) on a Gateway 450 MHz E-4200 serial processor, running Microsoft Windows NT 4.0.

The next example used real flight test data from the F-18 High Alpha Research Vehicle (HARV) to demonstrate the real-time parameter estimation method. Figure 6 shows the measured stabilator deflection for

this 14 second maneuver. Measured outputs are shown in Figure 7. The maneuver was a sequence of doublets implemented by the pilot from a steady trim condition at 20 deg angle of attack, 24,100 ft altitude, and Mach 0.37. Parameter estimates are plotted as a function of time in Figure 8, along with dashed lines indicating the $\pm 2\hat{\sigma}$ error bounds. Parameter estimates from standard batch time domain output error parameter estimation¹⁶ are plotted as solid lines for comparison. The real-time parameter estimation algorithm produced parameter estimates and standard errors that were in agreement with the batch time domain estimates after about 5 seconds, of which 1.5 seconds was steady trim with no information in the data. One cycle of the short period mode using the batch time domain parameter estimates was 7.5 seconds. Table 2 contains results at the end of the 14 second maneuver from batch time domain and real-time frequency domain parameter estimation.

As in the simulated data cases, the standard errors for the parameter estimates computed by the real-time parameter estimation algorithm were consistent with the accuracy of the parameter estimates throughout the maneuver. Specifically, the error bounds were large at the beginning of the maneuver, and smaller as more information was obtained from the data. Except for a few instances that are to be expected because of statistical variation, the standard errors were representative of the accuracy of the estimated parameters.

Sampling rate for the flight test data was 50 Hz, and the recursive Fourier transform updates were done at 25 Hz. The same implementation and computer as before were used. In this case, the real-time parameter estimation algorithm ran roughly 14 times faster than real time (1 second for a 14 second maneuver), because of the lower rate used for the recursive Fourier transform.

In the final example, control surface inputs measured in flight during a piloted longitudinal/lateral tracking task were applied to a nonlinear F-16 simulation^{11,14} with forward c.g. position (0.2 \bar{c}). Figure 9 shows the control surface inputs. The maneuver was initiated from a steady trim condition at 10 deg angle of attack, 10,000 ft altitude, and Mach 0.32. Simulated output data from the nonlinear simulation was corrupted with 20% white gaussian noise. The simulated noisy outputs are plotted in Figure 10. In this case, the lateral/directional linear model parameters were estimated in addition to the longitudinal model parameters from Eqs. (21)-(22).

For the lateral/directional aircraft dynamics, the state vector \mathbf{x} and input vector \mathbf{u} in Eq. (1) are defined by

$$\mathbf{x} = [\beta \quad p \quad r \quad \phi]^T \quad \mathbf{u} = [\delta_a \quad \delta_r]^T \quad (23)$$

System matrices containing the model parameters are:

$$\mathbf{A} = \begin{bmatrix} Y_\beta & \sin \alpha & -\cos \alpha & \frac{g}{V_t} \cos \theta \\ L_\beta & L_p & L_r & 0 \\ N_\beta & N_p & N_r & 0 \\ 0 & 1 & \tan \theta & 0 \end{bmatrix} \quad (24)$$

$$\mathbf{B} = \begin{bmatrix} 0 & Y_{\delta_r} \\ L_{\delta_a} & L_{\delta_r} \\ N_{\delta_a} & N_{\delta_r} \\ 0 & 0 \end{bmatrix} \quad (25)$$

Figure 11 shows time histories of selected longitudinal and lateral/directional model parameter estimates, with dashed lines indicating the $\pm 2\hat{\sigma}$ error bounds. Comparison values for the stability and control derivatives (plotted as solid lines) were calculated from the nonlinear simulation using central finite differences with a 1% perturbation size. Plots for the model parameters not shown were similar. As in the other examples, the performance of the real-time estimation algorithm was excellent, in spite of a relatively short (10 second) maneuver and low information content longitudinally. Parameter estimates converged to the finite difference values with appropriate standard error estimates. Cycle times for the short period and Dutch roll modes, based on the finite difference parameter values, were 3.8 seconds and 2.4 seconds, respectively. The real-time parameter estimation algorithm required 4 seconds to converge to the finite difference values for the model parameters using the tracking inputs measured in flight and plotted in Figure 9.

The sampling rate for the data was 80 Hz, and the recursive Fourier transform updates were done at 40 Hz. For the same implementation and computer as before, the real-time estimation algorithm for the longitudinal and lateral/directional models together ran roughly 8 times faster than real time (1.2 seconds for a 10 second maneuver).

Concluding Remarks

A technique was developed for estimating linear model parameters in real time, using an equation error formulation in the frequency domain with a recursive Fourier transform. Simulation and flight test examples demonstrated that the method gives accurate real-time estimates of model parameters and standard errors. The examples also showed that the advantages of this approach include automatic noise filtering, robustness to high noise levels and data dropouts, fixed memory requirements regardless of the time record length, no bias parameters to estimate, and good performance for low information content in the data. All of these favorable characteristics, as well as low computational requirements, follow from analyzing the data in the frequency domain with a recursive Fourier transformation using fixed discrete frequencies within the frequency range for the dynamic motion of interest.

The practical applicability of the method was demonstrated using a flight test data example, and a nonlinear simulation example using real flight test tracking inputs implemented by the pilot. Data information requirements for good parameter estimates were found to be low enough that they could be satisfied using ordinary pilot inputs measured in flight. The algorithm exhibited rapid convergence to accurate parameter values with standard errors that properly represented the accuracy of the parameter estimates. Typical convergence times were less than 1 cycle time of the dominant dynamic mode. No starting values were required for the parameter estimates, no tuning parameters had to be adjusted, and there was no temporal or spatial regularization during the parameter estimation. Parameter estimates and standard errors were based on measured data alone. The procedure was shown to have reasonable computational requirements, and ran much faster than real time, even when implemented in a high level language such as MATLAB.

The technique could be used for dimensional or non-dimensional parameter estimation, and could also be used with general nonlinear models, as long as the model is linear in the parameters. All states and inputs must be measured, but this should not be a problem in modern aircraft with continuous automatic feedback control, for which the method is intended.

The real-time parameter estimation technique studied in this work represents a fundamental building block for fulfilling the requirements of parameter estimation for adaptive or reconfigurable control. Future developments must focus on tracking rapid

time-varying linear model parameters resulting from changes in the flight condition, stores, configuration, remaining fuel, or from various types of failures, wear, or damage. In addition, there must be some work done to address the question of excitation input design when insufficient information content in the data precludes accurate parameter estimates.

References

1. Kaufman, H. "Assessment Study of the State of the Art in Adaptive Control and its Applications to Aircraft Control," Final Report, NASA Grant NAG-1-2075, NASA Langley Research Center, Hampton, VA, December 1998.
2. Bodson, M. "An Information-Dependent Data Forgetting Adaptive Algorithm," *Proceedings of the American Control Conference*, Seattle, WA, June 1995.
3. Chandler, P., Pachter, M., and Mears, M., "System Identification for Adaptive and Reconfigurable Control," *Journal of Guidance, Control, and Dynamics*, Vol. 18, No. 3, pp. 516-24, May-June, 1995.
4. Ward, D.G., Monaco, J.F., Barron, R.L., and Bird, R.A. "Self-Designing Controller - Design, Simulation, and Flight Test Evaluation," Final Technical Report for Contract F49620-94-C-0087, Barron Associates, Inc., Charlottesville, VA, November 1996.
5. Gelb, A., et al. *Applied Optimal Estimation*, The M.I.T. Press, Cambridge, MA, 1974.
6. Kokolios, A. "Use of a Kalman Filter for the Determination of Aircraft Aerodynamic Characteristics from Flight Test Data," AIAA Paper 94-0010, *32nd Aerospace Sciences Meeting & Exhibit*. Reno, NV, January 1994.
7. Bauer, J.E. and Andrisani, D. "Estimating Short-Period Dynamics using an Extended Kalman Filter," AIAA Paper AIAA-90-1277-CP, *Fifth Biannual Flight Test Conference*. Ontario, CA, May 1990.
8. Kaufman, H. "Aircraft Parameter Identification Using Kalman Filtering," *Proceedings of the National Electronics Conference*, Vol. XXV, pp. 85-9, December 1969.

9. Klein, V. "Two Biased Estimation Techniques in Linear Regression – Application to Aircraft," NASA TM 100649, July 1988.
10. Morelli, E.A. "In-Flight System Identification," AIAA paper 98-4261, *Atmospheric Flight Mechanics Conference*, Boston, MA, August 1998.
11. Stevens, B.L. and Lewis, F.L. *Aircraft Control and Simulation*, John Wiley & Sons, Inc. New York, NY, 1992.
12. Morelli, E.A. "High Accuracy Evaluation of the Finite Fourier Transform Using Sampled Data", NASA TM 110340, June 1997.
13. Klein, V. "Aircraft Parameter Estimation in Frequency Domain", AIAA paper 78-1344, *Atmospheric Flight Mechanics Conference*, Palo Alto, CA, August 1978.
14. Nguyen, L.T., et al. : "Simulator Study of Stall/Post-Stall Characteristics of a Fighter Airplane With Relaxed Longitudinal Static Stability", NASA TP 1538, December 1979.
15. *Using MATLAB, Version 5*, The MathWorks, Inc. Natick, MA, 1997.
16. Morelli, E.A. and Klein, V. : "Determining the Accuracy of Maximum Likelihood Parameter Estimates with Colored Residuals", NASA CR 194893, March 1994.

Table 1 F-16 Linear Simulation Results,
 $\alpha_o = 7$ deg, $h_o = 10,000$ ft, $M_o = 0.37$

Parameter	True Value	20% Noise Estimate (Std. Error)	50% Noise Estimate (Std. Error)
Z_α	-0.600	-0.624 (0.047)	-0.602 (0.132)
Z'_q	0.950	0.960 (0.016)	0.986 (0.044)
Z_{δ_e}	-0.115	-0.104 (0.017)	-0.134 (0.049)
M_α	-4.300	-4.197 (0.136)	-4.021 (0.354)
M_q	-1.200	-1.238 (0.045)	-1.200 (0.119)
M_{δ_e}	-5.157	-5.157 (0.048)	-5.246 (0.130)

Table 2 F18 HARV Flight Test Results,
 $\alpha_o = 20$ deg, $h_o = 24,100$ ft, $M_o = 0.34$

Parameter	Batch Time Domain Estimate (Std. Error)	Recursive Frequency Domain Estimate (Std. Error)
Z_α	-0.218 (0.040)	-0.209 (0.084)
Z'_q	1.047 (0.036)	1.074 (0.052)
Z_{δ_s}	-0.057 (0.046)	-0.041 (0.080)
M_α	-0.649 (0.044)	-0.509 (0.174)
M_q	-0.063 (0.032)	-0.177 (0.107)
M_{δ_s}	-1.257 (0.063)	-1.415 (0.165)

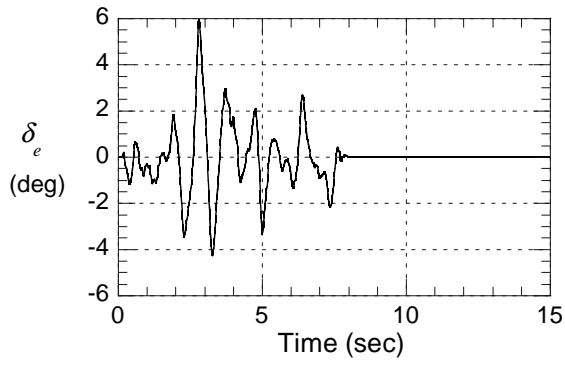


Figure 1 Elevator Input

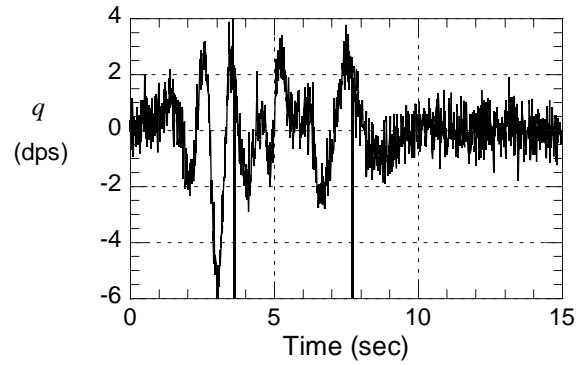


Figure 4 Simulated Measured Output, 50% Noise

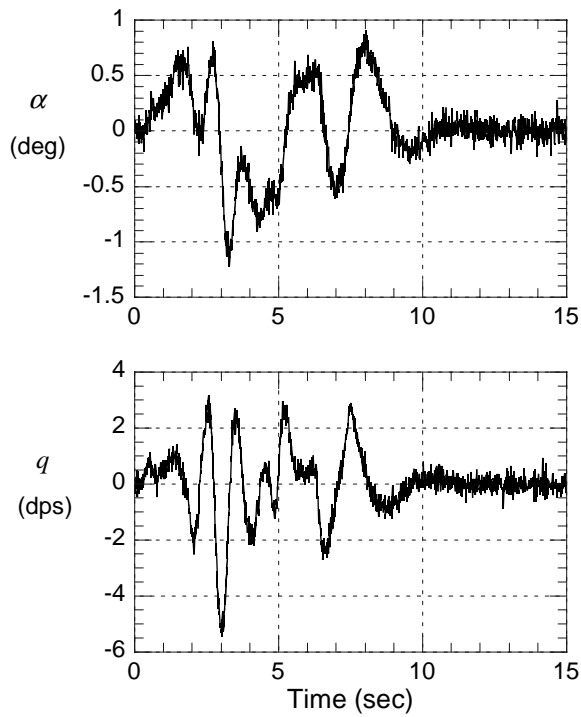


Figure 2 Simulated Measured Outputs, 20% Noise

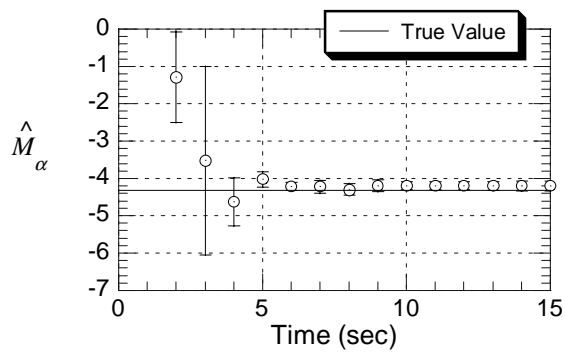


Figure 3 Parameter Estimation, 20% Noise

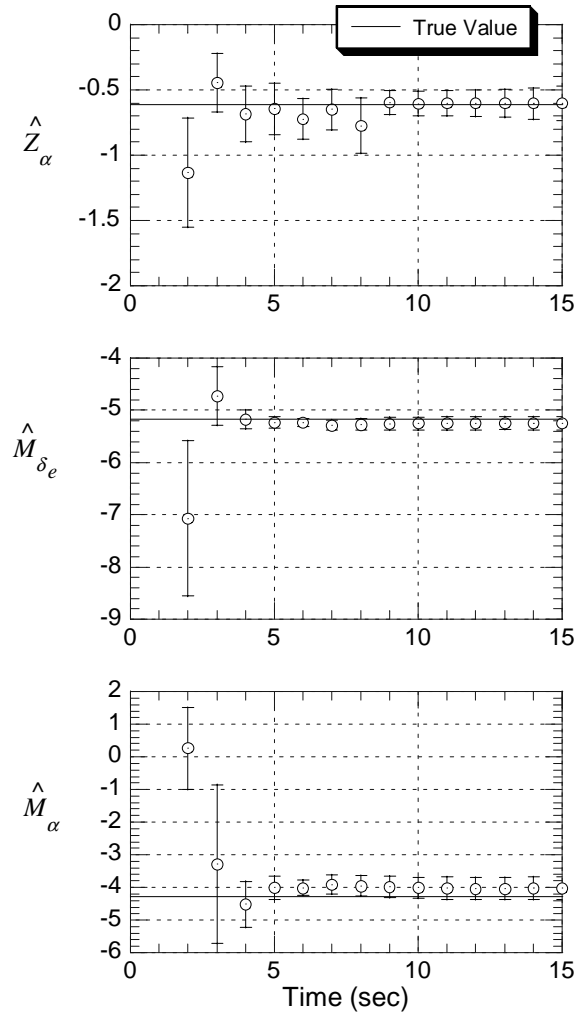


Figure 5 Parameter Estimation, 50% Noise

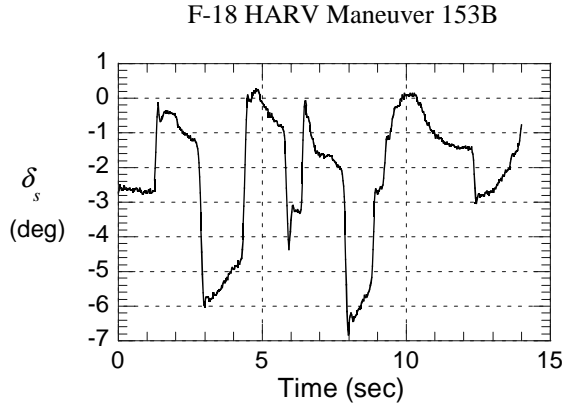


Figure 6 Stabilator Input

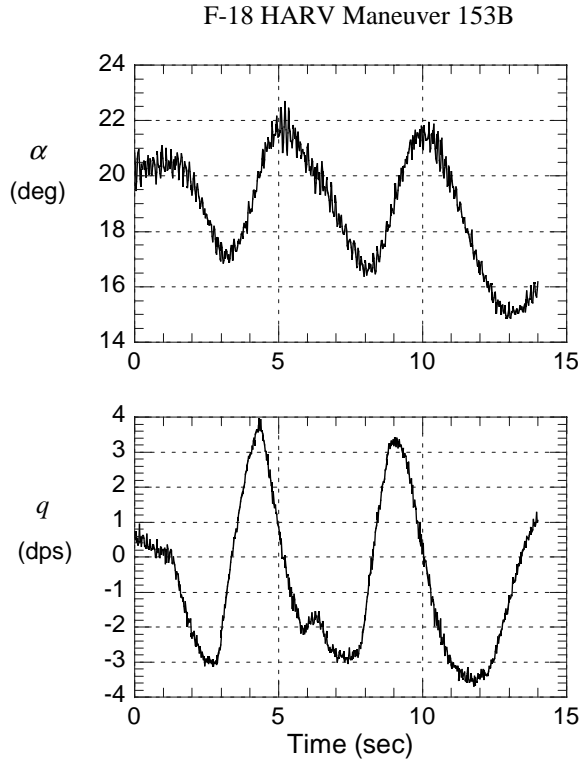


Figure 7 Measured Outputs

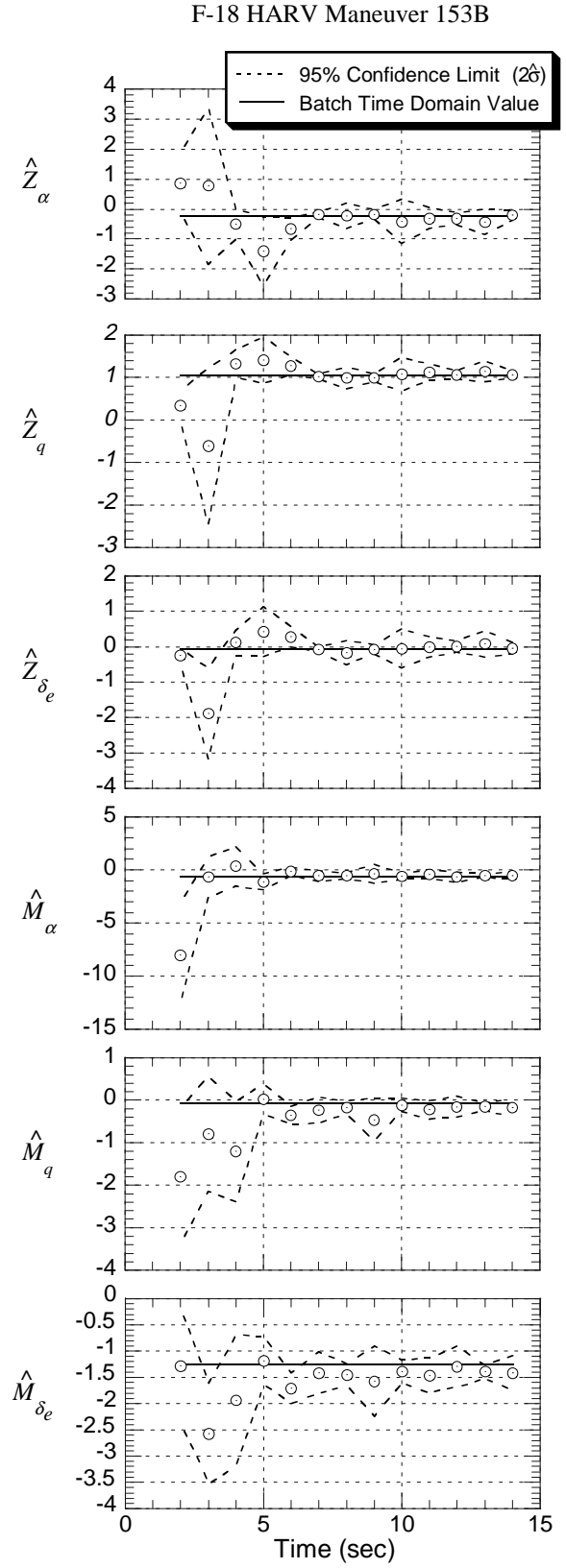


Figure 8 Parameter Estimation

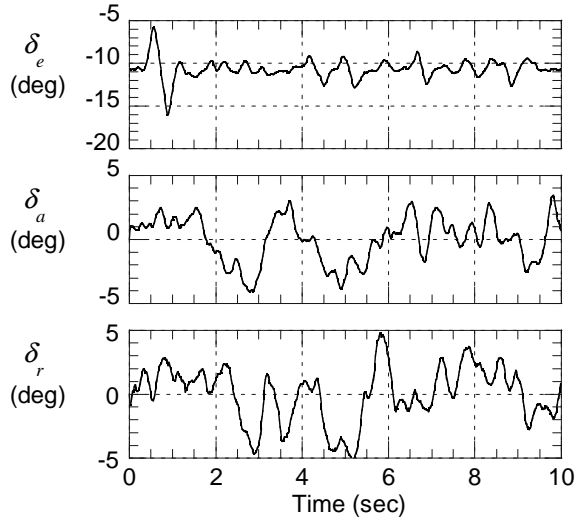


Figure 9 Tracking Inputs

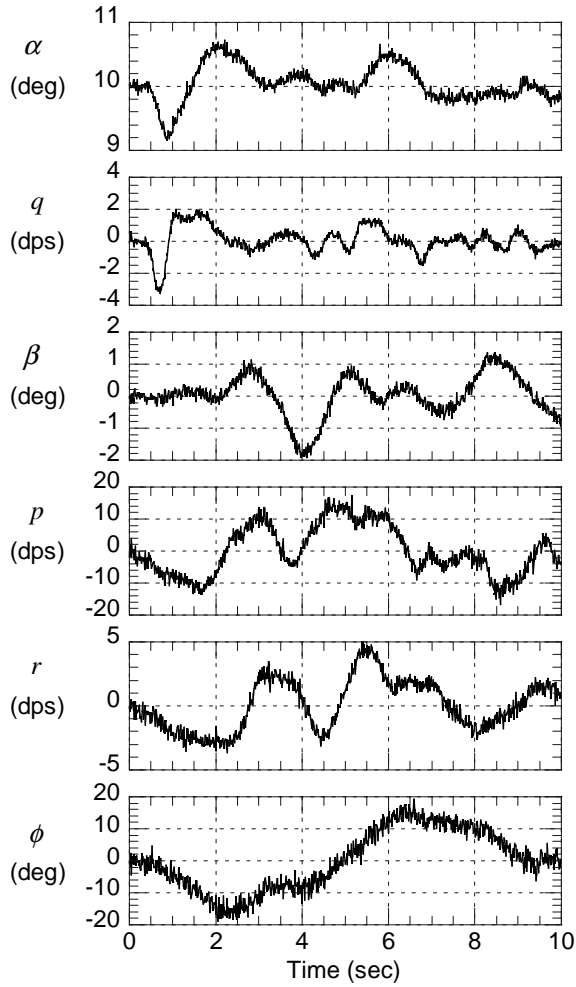


Figure 10 Simulated Measured Outputs, 20% Noise

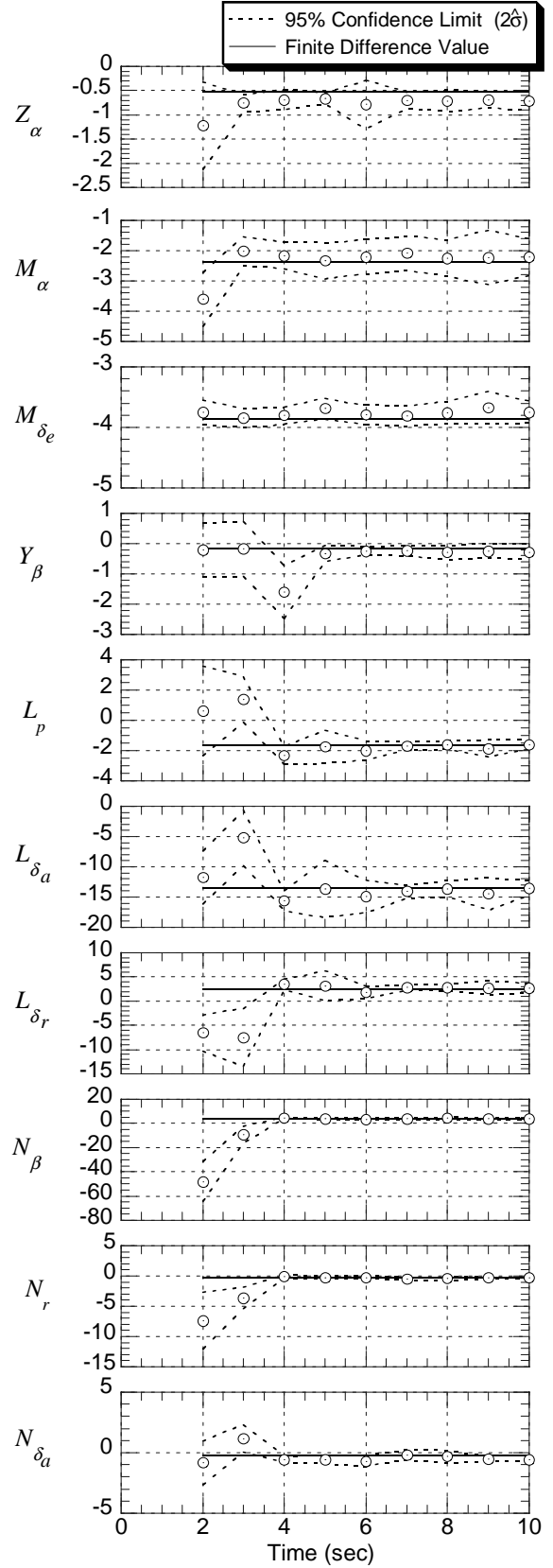


Figure 11 Parameter Estimation